AMERICAN SOCIETY FOR MICROBIOLOGY | Infection and Immunity®

BACTERIAL INFECTIONS

Histopathology of *Bordetella pertussis* in the Baboon Model

Lindsey I. Zimmerman,[a] James F. Papin,[b] Jason Warfel,[a] Roman F. Wolf,[b] Stanley D. Kosanke,[b] Tod J. Merkel[a]

[a]Division of Bacterial, Parasitic and Allergenic Products, Center for Biologics Evaluation and Research, U.S. Food and Drug Administration, Silver Spring, Maryland, USA

[b]Oklahoma Baboon Research Resource, Comparative Medicine, University of Oklahoma Health Sciences Center, Oklahoma City, Oklahoma, USA

ABSTRACT Pertussis is a severe respiratory disease caused by *Bordetella pertussis*. The classic symptoms of pertussis include paroxysmal coughing with an inspiratory whoop, posttussive vomiting, cyanosis, and persistent coryzal symptoms. Infants under 2 months of age experience more severe disease, with most deaths occurring in this age group. Most of what is known about the pathology of pertussis in humans is from the evaluation of fatal human infant cases. The baboon model of pertussis provides the opportunity to evaluate the histopathology of severe but nonfatal pertussis. The baboon model recapitulates the characteristic clinical signs of pertussis observed in humans, including leukocytosis, paroxysmal coughing, mucus production, heavy colonization of the airway, and transmission of the bacteria between hosts. As in humans, baboons demonstrate age-related differences in clinical presentation, with younger animals experiencing more severe disease. We examined the histopathology of 5- to 6-week-old baboons, with the findings being similar to those reported for fatal human infant cases. In juvenile baboons, we found that the disease is highly inflammatory and concentrated to the lungs with signs of disease that would typically be diagnosed as acute respiratory distress syndrome (ARDS) and bronchopneumonia. In contrast, no significant pathology was observed in the trachea. Histopathological changes in the trachea were limited to cellular infiltrates and mucus production. Immunohistostaining revealed that the bacteria were localized to the surface of the ciliated epithelium in the conducting airways. Our observations provide important insights into the pathology of pertussis in typical, severe but nonfatal pertussis cases in a very relevant animal model.

KEYWORDS nonhuman primates, *Bordetella pertussis*, histopathology, bronchiolitis, pneumonia, *Papio*, baboon, infant, juvenile, infectious disease

Pertussis is a severe respiratory disease caused by the Gram-negative bacterium *Bordetella pertussis* (1, 2). Despite high rates of vaccination, there has been a steady increase in reported pertussis cases in high-income countries, including the United States, over the last 20 years (https://www.cdc.gov/pertussis/surv-reporting.html). In 2012, the CDC reported 48,277 cases of pertussis in the United States (http://www.cdc.gov/pertussis/outbreaks/trends.html). It is likely that the number of reported cases significantly underestimates the burden of disease, as many cases go unreported (3). The severity of disease varies depending on the age, vaccination status, and history of exposure of the infected individuals and ranges from asymptomatic infection to severe disease requiring hospitalization (4). The classic symptoms of pertussis include paroxysmal coughing with an inspiratory whoop, posttussive vomiting, cyanosis, and persistent coryzal symptoms (3, 5). Young infants are much more likely to experience severe disease, with most hospitalizations and deaths occurring in children under 2 months of age (4, 6).

Much of what is known about the pathology of pertussis in humans is from the evaluation of fatal infant cases. Paddock et al. and others evaluated the pathology of

Received 12 July 2018 **Returned for modification** 7 August 2018 **Accepted** 13 August 2018

Accepted manuscript posted online 20 August 2018

Citation Zimmerman LI, Papin JF, Warfel J, Wolf RF, Kosanke SD, Merkel TJ. 2018. Histopathology of *Bordetella pertussis* in the baboon model. Infect Immun 86:e00511-18. https://doi.org/10.1128/IAI.00511-18.

Editor Guy H. Palmer, Washington State University

Address correspondence to Tod J. Merkel, tod.merkel@fda.hhs.gov.

fatal pertussis cases and found that each child experienced a descending respiratory infection that was characterized by pulmonary hemorrhage and edema, necrotizing bronchiolitis, and bronchopneumonia with damaged mucosa, denuded epithelium, and cilium loss in the trachea (7–9). While the pathology of these cases provides important insights into the damage inflicted on the respiratory system, these cases represent the end-stage pathology of the most severe infections. Although the majority of reported cases of pertussis in young infants are severe with significant morbidity, pertussis is not typically fatal in the United States, even in this young patient population. More typically, the patients eventually recover fully following a prolonged convalescent period (3, 5). Little is known about the pathology of these more typical cases of pertussis.

The baboon model of pertussis provides the opportunity to evaluate the histopathology of severe but nonfatal pertussis. The baboon model recapitulates the characteristic clinical signs of pertussis observed in humans, including leukocytosis, paroxysmal coughing, mucus production, heavy colonization of the airway, and transmission of the bacteria between hosts (10, 11). As in humans, the disease demonstrates age-related differences in severity. Five- to 6-week-old (infant) baboons experience very severe disease upon infection, often requiring euthanasia (12, 13). In contrast, 6- to 9-month-old (juvenile) baboons experience severe disease that lasts approximately 2 weeks, followed by a 2- to 3-week convalescence, resulting in a return to full health (10). We examined the histopathology of 5- to 6-week-old baboons that required euthanasia due to the severity of their disease following infection with *B. pertussis*, with the findings being similar to those reported for fatal human infant cases (7–9). In juvenile baboons, we found that the disease is highly inflammatory and concentrated to the lungs with signs of disease that would typically be diagnosed as acute respiratory distress syndrome (ARDS) and bronchopneumonia. Our observations provide important insights into the pathology of pertussis in typical severe but nonfatal pertussis cases in a very relevant animal model and suggest that many of the symptoms observed in human patients can be attributed to severely compromised lung function.

RESULTS

Histopathology observed in 5- to 6-week-old infant baboons. We previously conducted maternal vaccination studies in which we evaluated the ability of vaccination of pregnant female baboons with licensed and experimental vaccines to protect newborn infants from disease following exposure to *B. pertussis* (12, 13). These studies required inclusion of control animals whose mothers were not vaccinated during pregnancy. The infants born to unvaccinated mothers experienced severe disease following challenge that in some cases required humane euthanasia. Following euthanasia, tissue samples were collected from these animals, based on the reasoning that these samples allowed a comparison of severe infant baboon cases and fatal human infant cases for which histopathology is available. Histopathological evaluation was performed on samples from a total of five infant baboons that developed severe pertussis at between 2 and 13 days postchallenge. Upon gross examination, the lungs appeared very dense through the entire tissue and were mostly purple or dark in color. Hematoxylin-eosin (H&E) staining of the lungs (all lobes), nasal cavity, and trachea was performed. Microscopic examination revealed that the infection had a minimal impact on the nasal cavity and trachea (Fig. 1A). Instead, most of the damage was localized to the lungs, with all lobes of both lungs having equal involvement. The lungs revealed severe vascular leakage characterized by both acute hemorrhage and edema along with an intra-alveolar cellular influx consisting of both neutrophils and macrophages (Fig. 1B). Phosphotungstic acid-hematoxylin (PTAH) staining was also performed on these samples to visualize fibrin deposition. The PTAH stain revealed dense deposits of fibrin in the terminal (intra-alveolar) airways (Fig. 1C). The conducting airways revealed evidence of an acute necrotizing bronchitis/bronchiolitis often characterized by mucosal damage and an intraluminal influx of both neutrophils and macrophages, blood, and edematous fluid similar to that present in the terminal airways (Fig. 1D). In four of

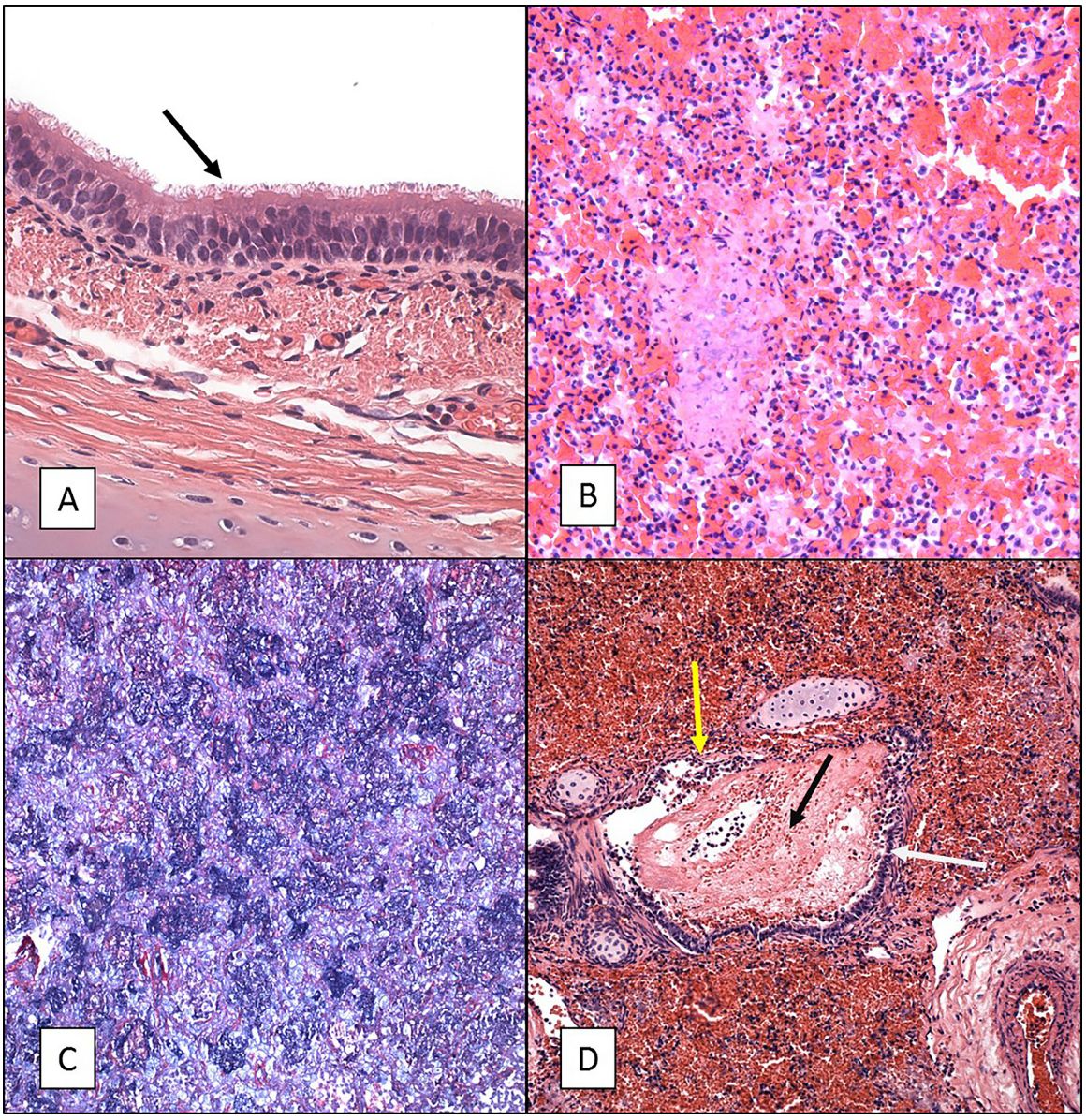

FIG 1 H&E and PTAH staining of tissue sections from 5- to 6-week-old baboons infected with *B. pertussis*. Five- to 6-week-old baboons were challenged with *B. pertussis*. H&E- and PTAH-stained slides were prepared from tissues as described in Materials and Methods. Representative images are presented. (A) Tracheal tissue stained with H&E showing intact cilia (arrow) and a normal appearance. (B) Lung tissue stained with H&E showing severe acute vascular leakage and mostly acute inflammation. (C) PTAH staining of lung tissue indicating intra-alveolar fibrin deposition in blue. (D) H&E staining of lung tissue showing necrotizing bronchitis/bronchiolitis. White arrow, bronchus, intact mucosa; yellow arrow, damaged mucosa; black arrow, intralumenal blood and edematous fluid. Magnifications, ×600 (A) and ×200 (B to D).

the five animals examined, Gram-negative bacterial aggregates, lymphoid cells, alveolar macrophages, and neutrophils were visualized in the terminal airways. Gram-positive bacterial aggregates were discovered in the lung tissue of the fifth animal, indicating that this animal had a secondary infection. This animal also had additional pathology more severe than that in the other four animals with thrombi and abscess formation with extensive parenchyma necrosis.

Histopathology observed in 6- to 9-month-old juvenile baboons. Juvenile baboons 6 to 9 months of age were challenged as described in Materials and Methods to study the pathology in severe but nonfatal pertussis. Baboons were euthanized, and tissue samples were collected at three time points postinfection: day 2 ($n = 3$), which represents early infection; day 7 ($n = 3$), which represents the peak of the infection; and

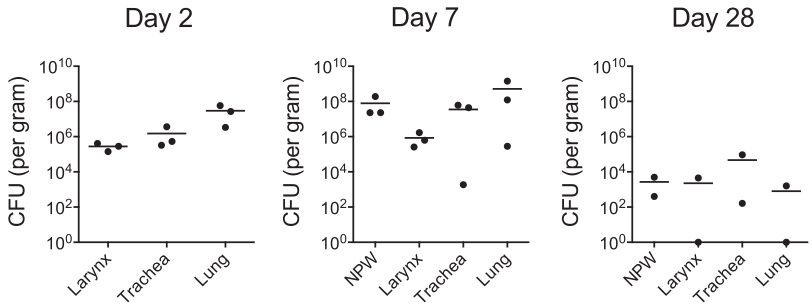

FIG 2 Numbers of bacterial CFU in airway tissues. Six- to 9-month-old baboons were challenged with *B. pertussis*, and samples were collected on days 2, 7, and 28 postchallenge. Tissues were weighed prior to homogenization in PBS, and the CFU were enumerated after dilution and plating on Regan-Lowe plates. The numbers of CFU per gram of tissue are reported. Direct comparison of bacterial numbers between tissue types is not possible due to the differences in the densities of the different tissues.

day 28 ($n = 2$), when the animals would be expected to be clearing the infection. For each animal, up to the time of euthanasia, the kinetics of infection of the nasopharynx, the white blood cell (WBC) counts in the circulation, and the outward clinical signs of disease were consistent with historical experience when animals allowed to progress through disease and convalescence were followed (data not shown) (10, 14, 15). In addition, tissue samples from euthanized uninfected controls ($n = 3$) were analyzed for comparison to those from the infected animals. The CFU from tissue samples collected from the larynx, trachea, and lung were enumerated (Fig. 2). At 2 and 7 days postinfection, we found that bacterial colonization was robust and diffuse throughout the respiratory tract. By day 28, the bacterial burden was notably reduced in all collected samples compared to that on days 2 and 7. These CFU data are consistent with our historical experience with pharyngeal wash specimens (10, 14, 15), in which animals clear infection in 4 to 6 weeks, indicating that these animals would likely have followed the same disease progression and would have cleared the infection. In addition to bacterial counts, pathology scores based on the histopathological observations were also used to quantify the severity of disease in the lungs and trachea of each animal at each time point (Fig. 3).

In all subjects, microscopic examination of the tracheal tissue samples with H&E staining revealed relatively normal-appearing tissue without significant pathology at any of the time points (Fig. 4A, B, and D). The primary finding was increased mucus and an influx of neutrophils and eosinophils in the mucosa and submucosa at day 7 compared to the findings for tracheal tissue sections from uninfected controls (Fig. 4C).

In contrast to the minor pathology observed in the trachea, lung tissue samples demonstrated marked disease progression over the course of infection when examined by H&E (Fig. 5 and 6), PTAH (Fig. 7), and trichrome (Fig. 8) staining. Day 2 lung tissue samples (Fig. 3 and 5B) exhibited evidence of marked vascular leakage compared to that for the uninfected controls (average pathology scores, 2.6 for day 2 and 0 for the controls), characterized by both intra-alveolar edema and hemorrhage with fibrin deposition (Fig. 5B) in the alveolar spaces. Lung consolidation was also a severe change relative to the findings for the uninfected controls (Fig. 5). In all lung tissue sections evaluated, evidence of bronchopneumonia and an influx of primarily neutrophils were noted, with a lesser number of macrophages, lymphocytes, and eosinophils being detected (Fig. 5). Some conducting airways had moderate luminal obstruction due to the presence of edematous fluid along with neutrophils and other cellular debris, which may have been partially associated with an acute necrotizing bronchitis/bronchiolitis and the sloughing of mucosal cells (Fig. 6A and B). A trichrome stain revealed minimal evidence of interstitial fibrosis (Fig. 8B).

By day 7 postinfection, vascular leakage and intra-alveolar edema had decreased compared to those on day 2 postinfection but were still moderate compared to those in the uninfected controls (Fig. 3 and 5C), but the fibrin deposition remained compa-

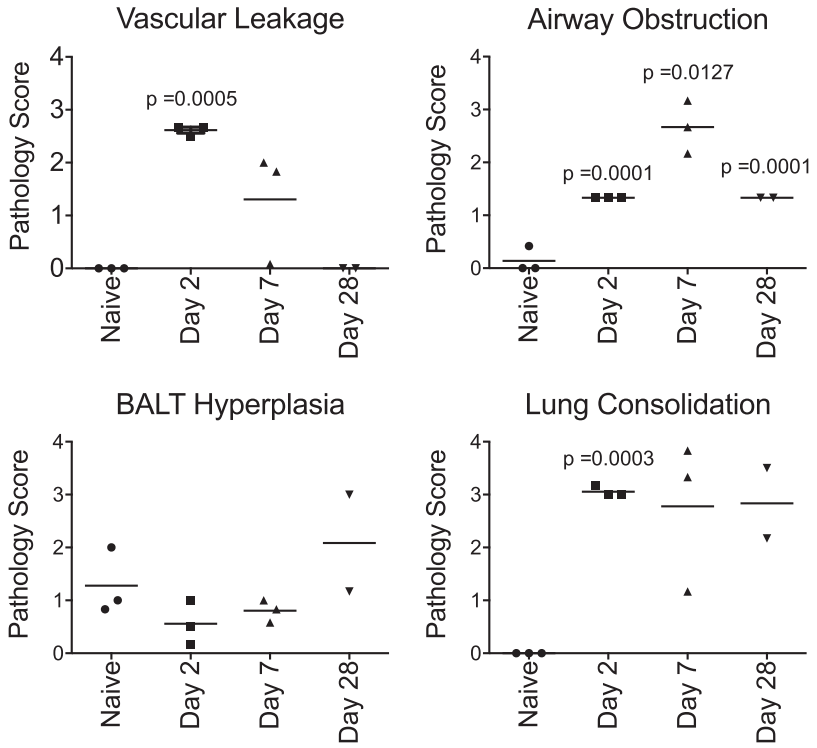

FIG 3 Pathology scores for 6- to 9-month-old baboons challenged with *B. pertussis*. Six- to 9-month-old baboons were challenged with *B. pertussis* as described in Materials and Methods. Animals were euthanized at days 2 ($n = 3$), 7 ($n = 3$), and 28 ($n = 2$). H&E-stained sections of the tracheal and lung tissues of all animals were examined by a board-certified veterinary pathologist and scored for vascular leakage, airway obstruction, BALT hyperplasia, and lung consolidation. Scores on a scale ranging from 0 to 4 were assigned as described in Materials and Methods. *P* values are reported relative to the naive group.

rable to that in the uninfected controls (Fig. 7B and C). The lung pathology revealed marked lung consolidation (average pathology score, 2.8) mostly composed of intra-alveolar cellular infiltrates. Again, neutrophils were the most prominent immune cell, with a lesser number of eosinophils, macrophages, and lymphocytes being observed (Fig. 5C). Conducting airway luminal obstruction was more severe on day 7 (average pathology score, 2.7) than on day 2, but the evidence of acute necrotizing bronchitis/bronchiolitis was similar on both days (Fig. 3, 5C, and 6C and D). A trichrome stain revealed minimal evidence of interstitial fibrosis (Fig. 8C).

By day 28 postinfection, the vascular leakage appeared to be resolved but lung consolidation remained marked compared to that in the uninfected controls (Fig. 3). Numerous areas of lung consolidation with cellular infiltrates were observed. In the terminal airways, the cellular infiltrates were mostly comprised of macrophages, with only occasional neutrophils and eosinophils being present. The conducting airways were moderately obstructed by sloughed mucosal cells, and infiltrates were mostly comprised of macrophages (Fig. 5D). Trichrome staining revealed evidence of prominent collagen deposition (Fig. 8D). In one of the two animals, bronchus-associated lymphoid tissue (BALT) hyperplasia was more prominent on day 28 than on day 2 or 7 (Fig. 3 and 5D). In the second animal, large areas of acute parenchymal necrosis with abscess formation were observed with heavy infiltration of neutrophils along with macrophages and lymphoid cells.

Fluorescent immunohistochemistry of the lung and tracheal tissue collected at 7 days postinfection was used to identify the location of *B. pertussis* bacterial cells by using an antibody that binds to a surface protein of the bacterium. In the lungs, the *B. pertussis* signal was found primarily in the bronchi either in mucous cellular debris that was obstructing the airways or on the mucosal surface but was not observed in the

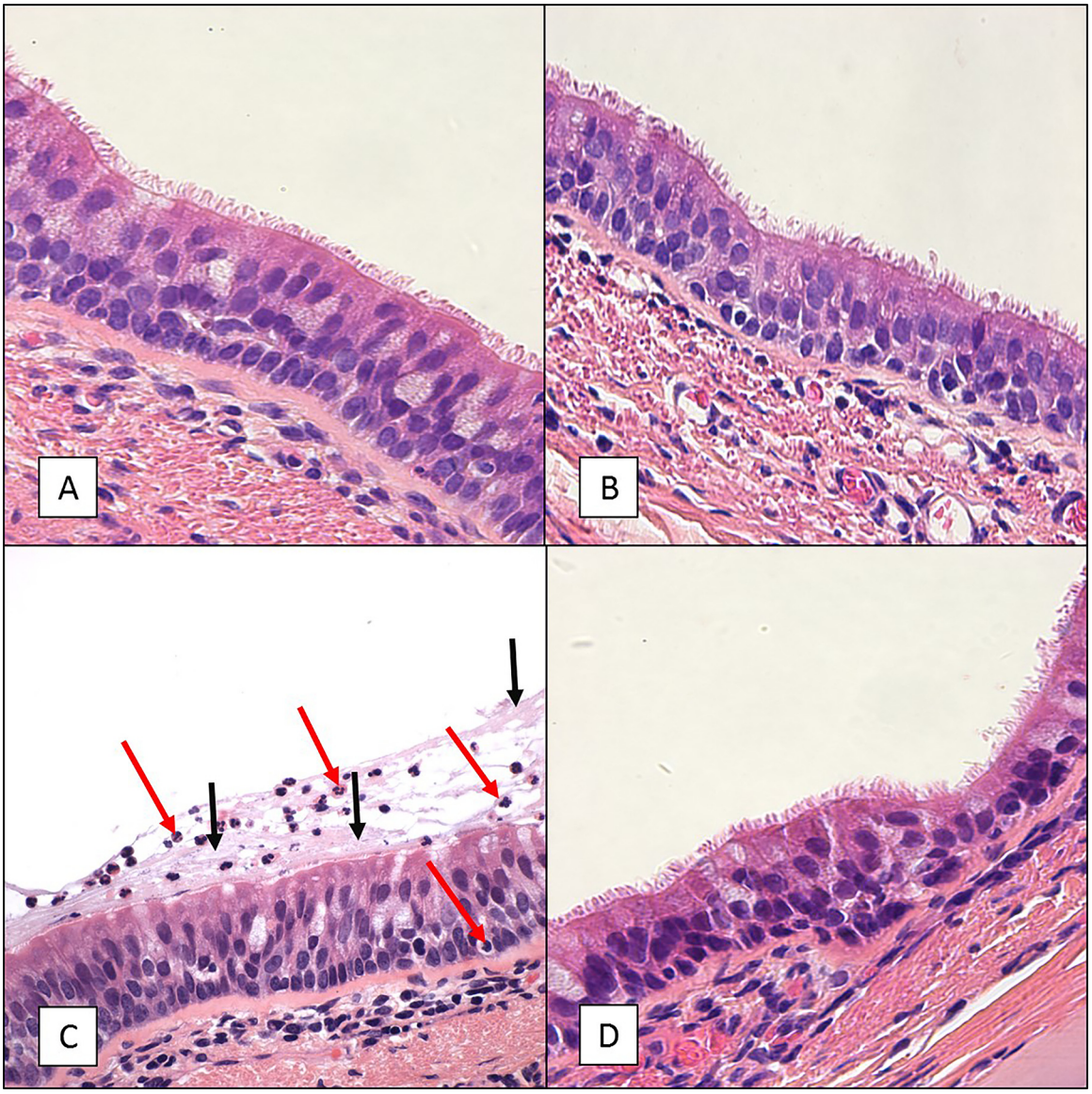

FIG 4 H&E staining of tracheal tissue sections from 6- to 9-month-old baboons infected with *B. pertussis*. Six- to 9-month-old baboons were challenged with *B. pertussis*. Tracheal tissue samples were collected on days 2, 7, and 28 postchallenge, and H&E-stained slides were prepared as described in Materials and Methods. Representative images are presented. (A) Sample collected from an uninfected baboon. (B) Sample collected from a baboon at day 2 postchallenge. (C) Sample collected from a baboon at day 7 postchallenge demonstrating influx of neutrophils (red arrows) and excess mucus (black arrows) lining the mucosa. (D) Sample collected from a baboon at day 28 postchallenge. Magnifications, ×600.

alveolar spaces (Fig. 9). A lack of *B. pertussis* staining in the underlying connective tissue suggested that there was no bacterial invasion of tissues beyond the mucosal surface. Similarly, in the trachea, *B. pertussis* staining was associated mainly with the mucosal surface of the airway (Fig. 10). In the trachea, *B. pertussis* staining was also observed on the mucosal surface of submucosal ducts but was not observed in any other underlying tissue.

DISCUSSION

Much of our understanding of pertussis pathology in humans is based on the histopathology of samples collected from fatal infant cases (7–9, 16). Although this information provided a critical understanding of the pathology of the most severe cases of pertussis, it may not accurately reflect the pathology of the more common cases of pertussis in older infants and children that are severe but not fatal. The baboon model

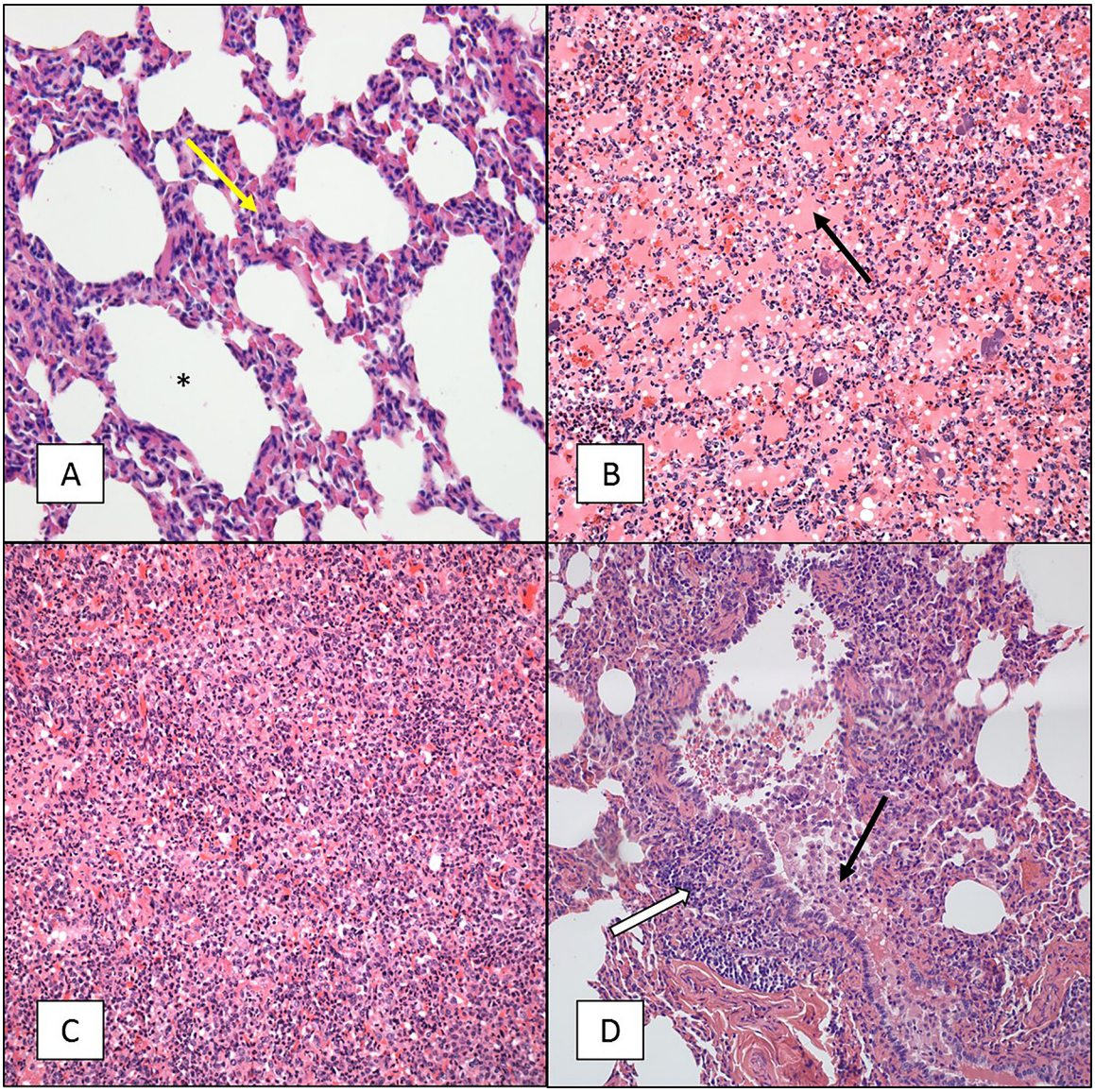

FIG 5 H&E staining of lung tissue sections from 6- to 9-month-old baboons infected with *B. pertussis*. Six- to 9-month-old baboons were challenged with *B. pertussis*. Lung tissue samples were collected on days 2, 7, and 28 postchallenge, and H&E-stained slides were prepared as described in Materials and Methods. Representative images are presented. (A) Sample collected from an uninfected baboon. Note that the alveoli (*) are empty and there are few inflammatory cells in the interalveolar septum (yellow arrow). (B) Sample collected from a baboon at day 2 postchallenge revealing marked vascular leakage consisting primarily of intra-alveolar edema (which stains pink; black arrow). (C) Sample collected from a baboon at day 7 postchallenge revealing moderate vascular leakage and marked lung consolidation. Note the almost complete loss of alveolar space and the influx of inflammatory cells and edema. (D) Sample collected from a baboon at day 28 postchallenge revealing marked lung consolidation and BALT hyperplasia (white arrow) with the conducting airways obstructed by macrophages and sloughed mucosal epithelial cells (black arrow). Magnifications, ×200.

of pertussis allowed us to address this gap in our knowledge by providing pathology samples from multiple time points from animals exhibiting severe but not fatal disease. This was achieved by challenging animals following a protocol that has been demonstrated to cause severe disease with symptoms that recapitulate the classic symptoms observed in humans, including a convalescent period with eventual clearance of the organism and a return to good health. In this study, we euthanized animals at defined time points following challenge to evaluate the pathology. For each animal, up to the time of euthanasia, the kinetics of infection of the nasopharynx, the WBC counts in the circulation, and the outward clinical signs of disease were consistent with historical experience with animals allowed to progress through disease and convalescence (10,

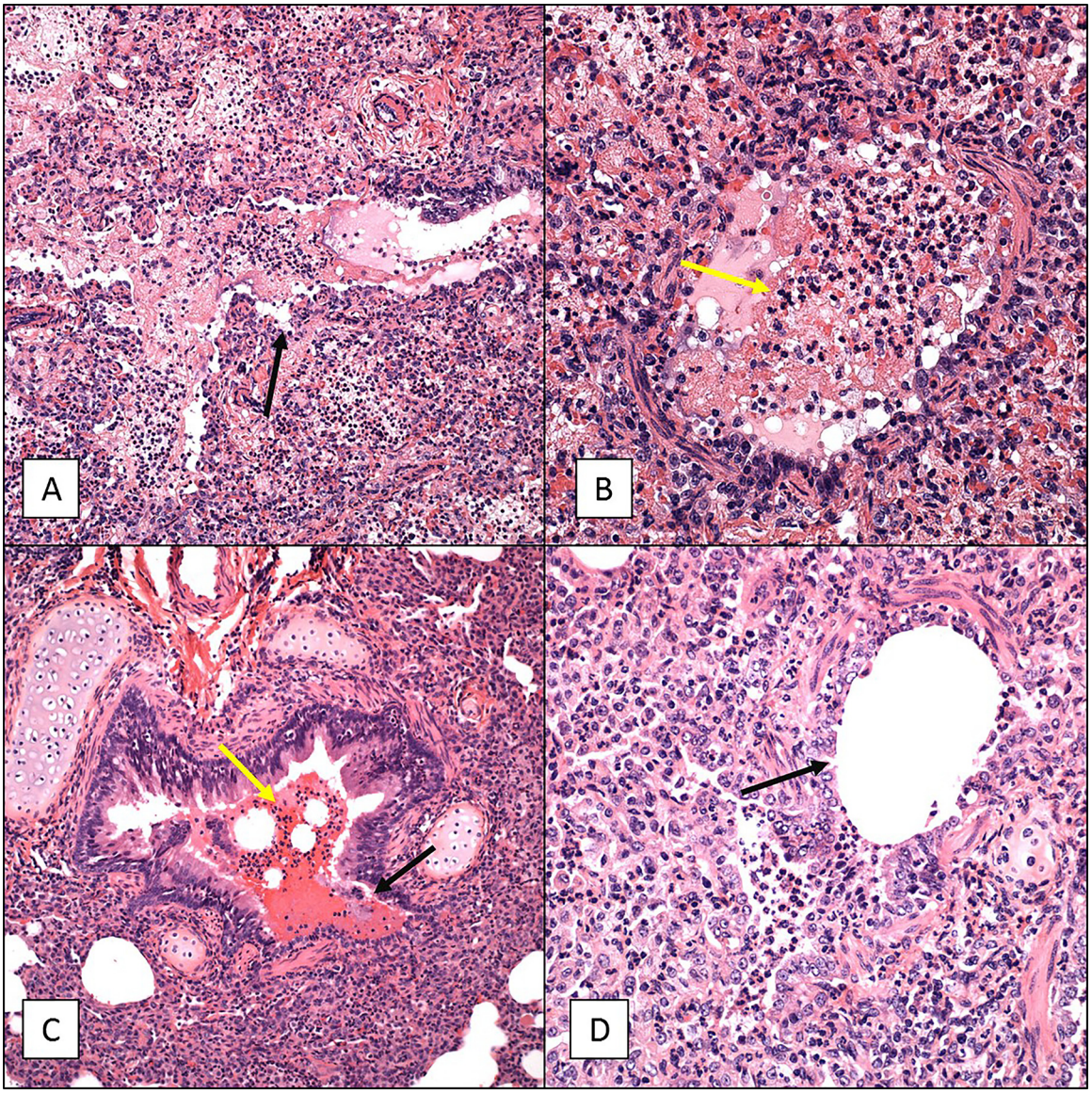

FIG 6 Necrotizing bronchitis/bronchiolitis of 6- to 9-month-old baboon lungs infected with *B. pertussis*. Six- to 9-month-old baboons were challenged with *B. pertussis*. Lung tissue samples were collected on days 2 and 7, and H&E-stained slides were prepared as described in Materials and Methods. Representative images showing necrotizing bronchitis/bronchiolitis are presented. (A and B) Samples collected from a baboon at day 2 postchallenge. (C and D) Samples collected from a baboon at day 7 postchallenge. For all panels, the lumen of the bronchus is almost completely filled with edema, fibrin, and inflammatory cells (yellow arrows), and the mucosa (black arrows) has been severely damaged. Magnifications, ×200 (A and C) and ×400 (B and D).

14, 15). Therefore, it is reasonable to assume that these animals would have followed the same progression of disease and convalescence that is typically observed in baboon pertussis challenges.

Infant baboons that were euthanized because of severe pertussis infection exhibited a pathology similar to that observed in fatal human cases of *B. pertussis* (7–9, 16). In both hosts, subjects experienced descending disease, with pulmonary hemorrhage, edema, and fibrin deposits obstructing the terminal airways. The pathology observed in the infant baboons resembled that in the early stages of acute respiratory distress syndrome (ARDS) with mild evidence of acute nasopharyngitis and bronchopneumonia. In the fatal human cases, the trachea revealed a partial loss of the ciliated epithelium and damaged mucosa, while the infant baboon cases essentially had normal tracheas. This difference in pathology could be due to inherent differences between

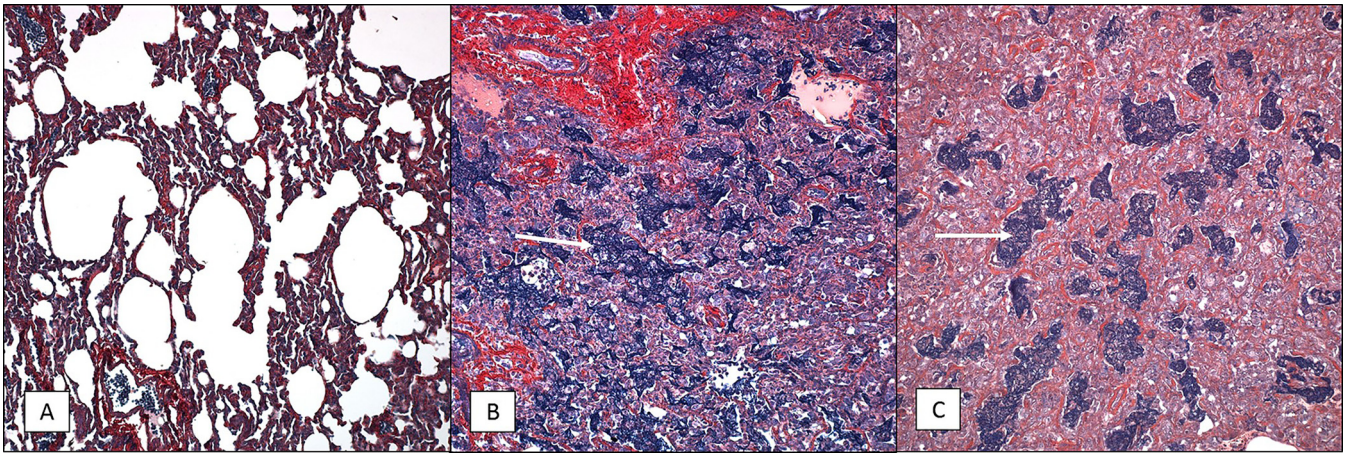

FIG 7 PTAH staining of lung tissue sections from 6- to 9-month-old baboons infected with *B. pertussis*. Six- to 9-month-old baboons were challenged with *B. pertussis*, and PTAH-stained slides were prepared as described in Materials and Methods. Representative images are presented. Lung tissue samples were collected from uninfected animals (A) and from infected animals at day 2 postchallenge (B) and day 7 postchallenge (C), and intra-alveolar fibrin deposition is shown in dark blue/purple (white arrows). Magnifications, ×200.

humans and baboons or may be due to differences in the severity of the disease. Although the infant baboons were comparable in age to the human infant cases, ethical constraints required that these animals be humanely euthanized as soon as it became clear that the animals were experiencing severe clinical disease. Therefore, the pathology in these infant baboon cases would not be expected to be as severe as that observed in human infant cases in which the individuals succumbed to infection. The overall similarity in the pathology observed in the fatal human infant cases and the severe baboon infant cases provides confidence that the baboon model can provide useful information about the pathology of disease in nonfatal cases for which human pathology data are not available.

When juvenile baboons were challenged with *B. pertussis*, most of the lung tissue samples revealed the bacteria to be present on the ciliated surface of the mucosa, suggesting that during infection *B. pertussis* largely colonizes the extracellular space on the surface of the ciliated epithelium of the respiratory tract. The diagnosis, based on the histopathology for all animals, was ARDS and bronchopneumonia. The changes noted in the trachea were limited to excess mucus production and transmural inflammatory infiltrates consisting primarily of neutrophils at day 7. The lack of significant pathology in the trachea is striking. In numerous studies utilizing polarized tracheal or bronchial tissue culture or explanted nasal turbinate, adenoid, or tracheal organ tissue culture, the ciliated epithelial tissues demonstrated ciliostasis, a loss of cilia, cell extrusion, and sloughing of cells when infected with *B. pertussis* (17–19). Similar damage was reported in a study examining nasal epithelial biopsy samples taken from children with pertussis (20). It is possible that this represents a difference between baboons and humans; however, in a study conducted in the prevaccine era, autopsy samples collected from three children at between 1 and 3 years of age that died from pertussis were examined. The ciliated tracheal epithelia were intact with some mucus production, despite the presence of large numbers of bacterial cells in foci throughout the tracheas (21). These findings are similar to our observations in the infected baboon tracheas.

In contrast to the trachea, significant pathology was observed in the lungs. Lung consolidation was rated as marked to severe at both day 2 and day 7. Vascular leakage was marked at day 2 and only moderate at day 7. Deposits of fibrin were evident upon staining with PTAH at both day 2 and day 7. In the conducting airways (bronchi and bronchioles), transmural inflammatory infiltrates consisting primarily of neutrophils with few to no macrophages were observed at days 2 and 7. Partial to complete luminal obstruction due to an influx of inflammatory cells comprised mostly of neutrophils and

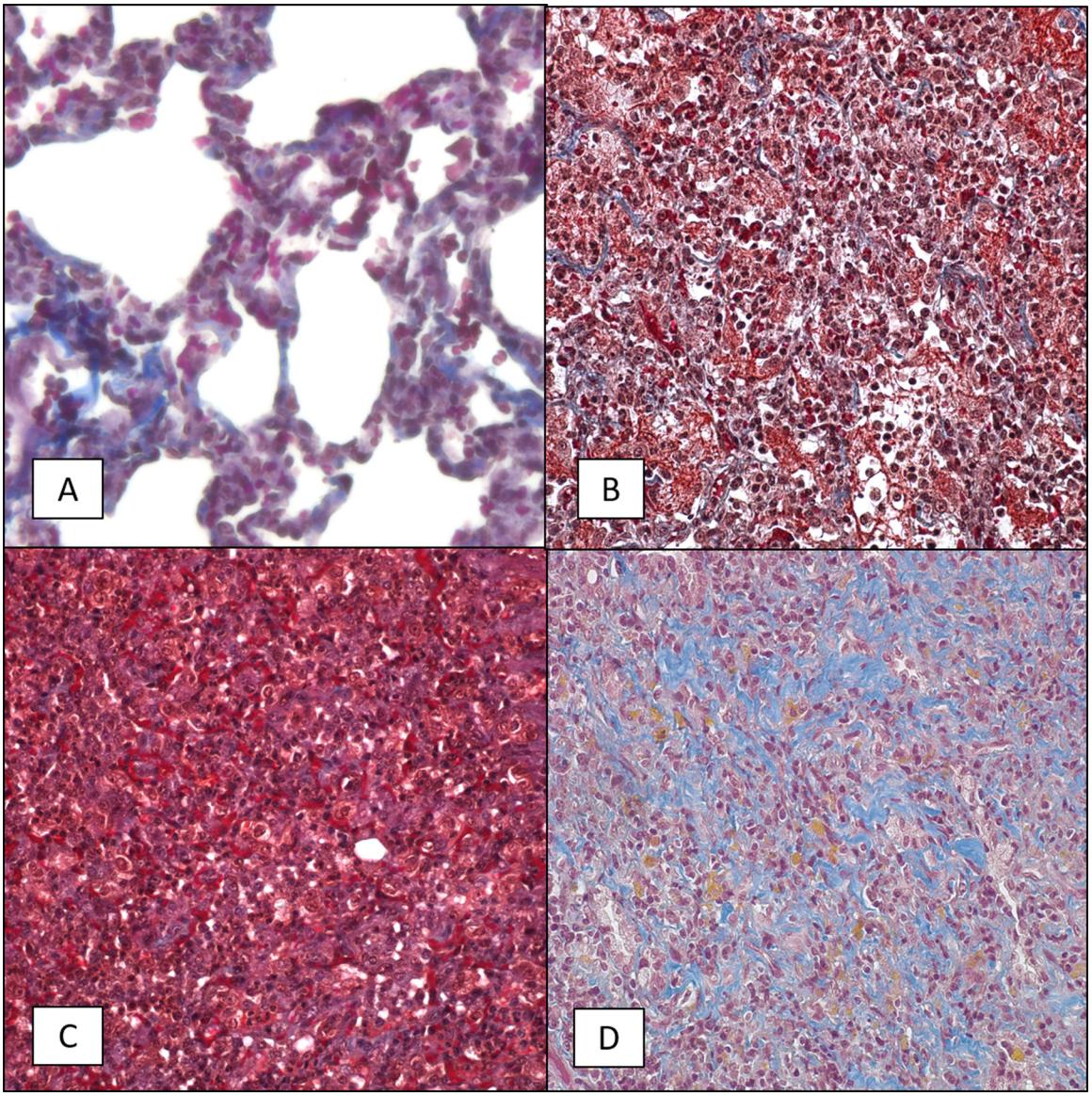

FIG 8 Trichrome staining of lung tissue sections from 6- to 9-month-old baboons infected with *B. pertussis*. Six- to 9-month-old baboons were challenged with *B. pertussis*, and trichrome-stained slides were prepared as described in Materials and Methods. Representative images of lung tissue samples collected from uninfected animals (A) and from infected animals at day 2 postchallenge (B), day 7 postchallenge (C), and day 28 postchallenge (D) showing collagen deposition in blue are presented. Magnifications, ×400.

sloughed mucosal epithelial cells was observed. At times this included evidence of acute necrotizing bronchitis/bronchiolitis. The observation of cellular infiltrates consisting primarily of neutrophils is in marked contrast to the observation in fatal human infant cases, in which cellular infiltrates were comprised primarily of macrophages. This difference probably reflects differences in the stage of disease progression rather than differences in disease between the two species. Late in infection in the baboon model, by day 28, neutrophils were replaced by macrophages. It is likely that the same progression occurs in human cases, with neutrophils infiltrating in large numbers early in the infection, followed by the recruitment of macrophages during later stages of the disease. Our work in the baboon model as well as extensive work in the mouse model and supporting serological studies in humans has resulted in the hypothesis that Th1 and Th17 responses resulting in the induction of opsonizing antibodies and the recruitment of neutrophils to the site of infection are required for the effective clearance of pertussis from the airway (15, 22–29). The observation, reported here, that

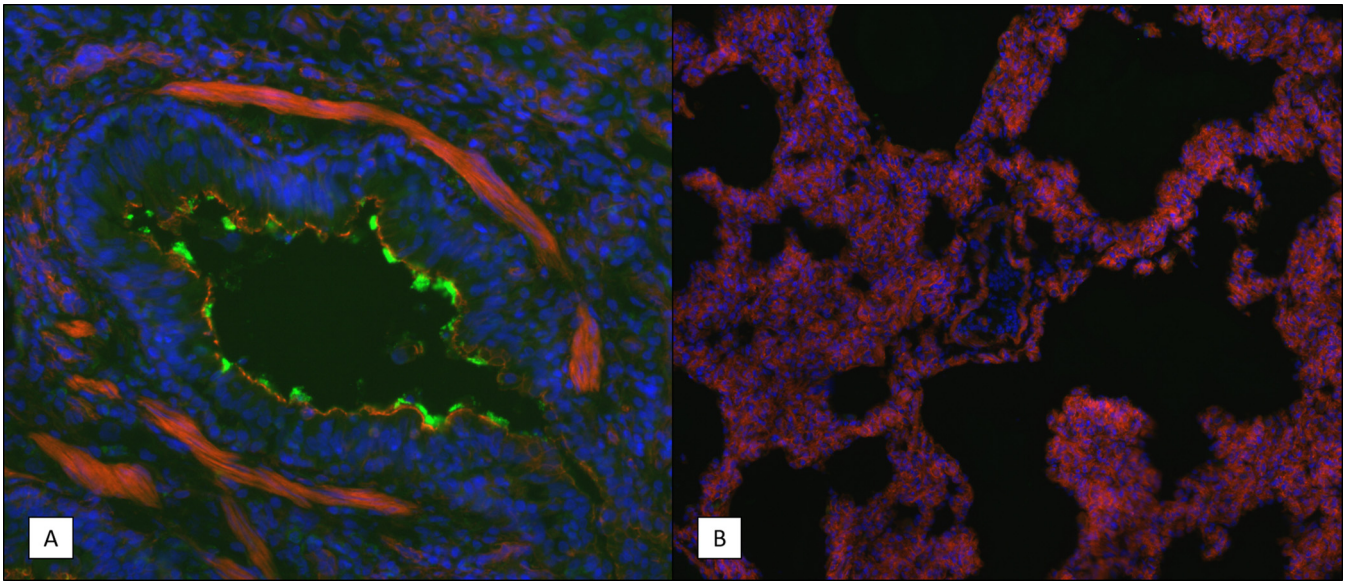

FIG 9 Immunohistochemistry (IHC) staining of *B. pertussis* in lung tissue sections. Frozen lung tissue sections were prepared from infected animals on day 7 postchallenge as described in Materials and Methods. *B. pertussis* bacteria were visualized using rabbit polyclonal antibodies specific for a surface-exposed antigen. Representative images are shown. Blue indicates the DAPI staining of the nucleus, red indicates the staining of F actin, and the green in panel A indicates *B. pertussis* bacterial cells. (A) Bronchiole showing bacteria lining the mucosal surface. (B) Alveolar space of an infected animal showing an absence of bacteria. Magnifications, ×200 (A) and ×100 (B).

neutrophils infiltrate the respiratory mucosa and luminal space in the airway early in infection provides important support for that hypothesis.

Although all the classic hallmarks of inflammation are not present, the response to *B. pertussis* infection observed in the lungs of the juvenile baboons is best described as

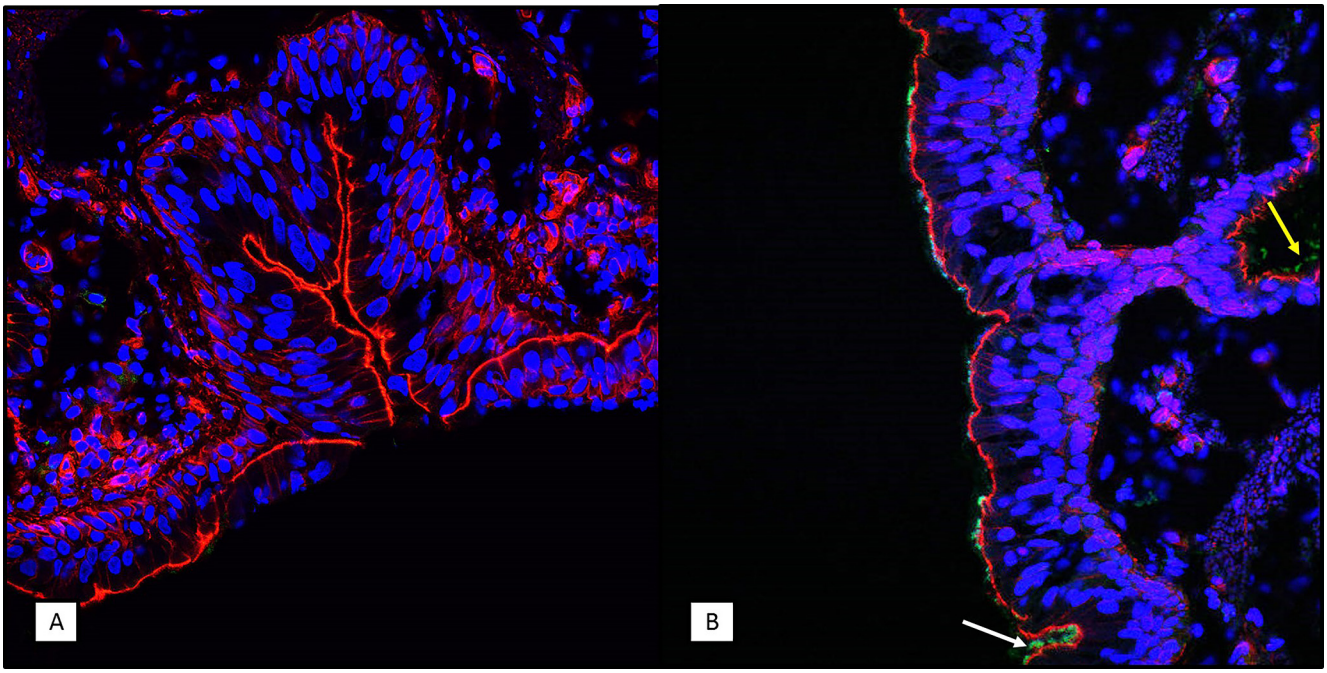

FIG 10 Immunohistochemistry (IHC) staining of *B. pertussis* in tracheal tissue sections. Frozen tracheal tissue sections were prepared from uninfected animals (A) and from infected animals on day 7 postchallenge (B), as described in Materials and Methods. *B. pertussis* bacteria were visualized using rabbit polyclonal antibodies specific for a surface-exposed antigen. Representative images are shown. Blue indicates the DAPI staining of the nucleus, red indicates the staining of F actin, and the green in panel B indicates *B. pertussis* bacterial cells. Bacteria are observed on the mucosal surface in the tracheal lumen (white arrow) and submucosal ducts (yellow arrow). Magnifications, ×400.

an inflammatory response in which the alveolar space within significant areas of the lungs first fills with fluid, followed by cellular infiltration. Although this inflammatory response may ultimately result in clearance of the infection, many of the symptoms associated with acute pertussis could be attributed to the decreased lung function resulting from the consolidation of large areas of the lung due to this inflammatory response.

Although small numbers of bacteria were still present in both animals examined at day 28, the lungs appeared to be recovering from infection at this point. H&E-stained sections appeared mostly normal, although in one of two animals, significant BALT hyperplasia was evident. This likely reflects a dramatic expansion of host immune cells in response to the infection. Staining of day 28 lung tissue with trichrome indicated that the intra-alveolar fibrin deposition seen at days 2 and 7 leads to the extensive deposition of collagen observed at day 28. Anecdotal evidence indicates that some individuals that have recovered from severe cases of pertussis relapse when subsequently exposed to mild respiratory viral infections (16). If the collagen deposition in the lung that we observed at day 28 in juvenile baboons accurately reflects the condition of the lungs in humans following recovery from a severe case of pertussis, it may explain the increased sensitivity to subsequent respiratory assault. Until the collagen is remodeled to restore normal tissue, the decreased lung capacity likely exacerbates otherwise mild lung infections.

Taken together our results indicate that in severe but nonfatal cases of pertussis, the infection involves the lung to a much greater extent than previously suspected and involves the upper airway to a lesser extent. Although the impact of the infection involves both the conducting (trachea, bronchi, and bronchioles) and gas exchange terminal (alveolar) areas of the lung, the bacteria appear to be concentrated in the conducting airways. Immunostaining for bacteria revealed bacteria adhering to the mucosal surface in the trachea, bronchi, and bronchioles, but bacteria were not routinely observed in the alveolar space. This is consistent with the known ability of *B. pertussis* to adhere to ciliated epithelial surfaces.

The results of this study reveal for the first time the severity of the pathology in the lungs in severe but nonfatal cases of pertussis. In addition to providing important insights into pertussis disease, this study provides a useful model for examining the ability of vaccines and therapeutics to prevent or reduce the observed pathology.

MATERIALS AND METHODS

Ethics statement. Animal procedures were performed in a facility accredited by the Association for Assessment and Accreditation of Laboratory Animal Care International in accordance with protocols approved by the University of Oklahoma Health Sciences Center Animal Care and Use Committee and the principles outlined in the *Guide for the Care and Use of Laboratory Animals* by the Institute for Laboratory Animal Resources, National Research Council (30).

Bacterial strains. *Bordetella pertussis* strain D420 was provided by the Centers for Disease Control and Prevention. Bordet-Gengou (BG) agar plates were prepared with BG agar (Becton Dickinson, Sparks, MD) supplemented with 1% proteose peptone (Becton Dickinson) and 15% defibrinated sheep blood. Regan-Lowe plates were prepared from Regan-Lowe charcoal agar base (Becton Dickinson) with 10% defibrinated sheep blood and 40 μg/ml cephalexin.

Infection of baboons. Baboons (*Papio anubis*) were obtained from the Oklahoma Baboon Research Resource. All baboons were outbred, were free of tuberculosis, and had normal leukocyte concentrations (range, 5,000 to 12,000/mm^3) at the time of infection. Infection of baboons and sample collections were performed at the University of Oklahoma Health Sciences Center using previously published procedures (10, 12, 13). Briefly, neonatal baboons 5 to 6 weeks of age were challenged with a freshly prepared inoculum at a concentration of 10^8 bacteria/ml. Following anesthesia with ketamine and acepromazine, the baboons were intubated with a 3.0-mm (inner diameter) endotracheal tube, and 0.5 ml of inoculum was delivered through the tube to the proximal trachea. Subsequently, 0.25 ml of inoculum was administered into each naris using a 22-gauge flexible Teflon catheter. Animals were placed into a sitting position for 3 min prior to being returned to the cage, where they were observed until fully recovery from anesthesia. Juvenile baboons 6 to 9 months of age were challenged with the same procedures, with the exception that the inoculum concentration was 10^9 bacteria/ml and 1 ml was administered intratracheally and 0.5 ml was administered into each naris as previously published (10).

Evaluation of animals. Baboons were anesthetized with ketamine. Whole-blood specimens were evaluated for the number of circulating white blood cells by complete blood count. Each nasal pharynx was flushed with 0.5 ml of phosphate-buffered saline (PBS), using a 22-gauge/3.2-cm intravenous

catheter. The recovered nasopharyngeal wash (NPW) samples from both nares were combined, and 100 μl of the recovered sample was divided, serially diluted in PBS, and plated onto Regan-Lowe plates. The CFU were enumerated after incubation at 37°C for 4 to 5 days. Infection with *B. pertussis* was confirmed by examining the colony morphology and hemolysis on BG blood agar plates and PCR amplification of IS*481*, a genomic insertion site that is specific for *B. pertussis*.

Tissue collection. Uninfected baboons and baboons experimentally infected with *B. pertussis* were euthanized by intravenous overdose of sodium pentobarbital due to severe disease associated with pertussis (infant baboons) or at days 2, 7, and 28 following challenge (juvenile baboons). Larynx, tracheal, and lung tissue samples were collected immediately following euthanasia for histopathology, immunohistochemistry, and enumeration of the CFU. For each evaluation, sections were collected from the upper and lower half of the trachea. Random sections were collected from each lobe of the lung.

Tissue CFU. For each animal, one piece of larynx tissue, two pieces of tracheal tissue (upper and lower), and six pieces of lung tissue (two each from the upper, middle, and lower lobes) were weighed, placed in PBS, and homogenized. Homogenized samples were serially diluted in PBS and plated onto Regan-Lowe plates. The CFU were enumerated after incubation at 37°C for 4 to 5 days.

Histopathology. Tissues for histopathology were fixed with 10% buffered formalin, embedded, and sectioned onto slides for staining with hematoxylin and eosin (H&E), phosphotungstic acid-hematoxylin (PTAH), or trichrome stain. PTAH is a specialized stain used to demonstrate fibrin (which stains a dark blue) in histopathology sections. The trichrome stain is a specialized stain used to identify collagen (which stains light blue) in tissue sections. Stained slides were then visualized using an Olympus BX40 or Leica DMi8 microscope. The slides were evaluated by a board-certified veterinary pathologist and scored for vascular leakage, lung consolidation, conducting airway obstruction, and BALT hyperplasia. Scoring was performed by assigning a value on a scale of from 0 to 4. For the vascular leakage and lung consolidation, the scoring system was based upon the percentage of terminal airways involved, as follows: 0 was normal (0%), 1 was mild involvement (1 to 25%), 2 was moderate involvement (26 to 50%), 3 was marked involvement (51 to 75%), and 4 was severe involvement (greater than 75%). For airway obstruction and BALT hyperplasia, the scoring system was based upon the same percentages listed above for the terminal airways but for those conducting airways involved. Lung tissue from three uninfected baboons was analyzed similarly.

Fluorescent immunohistochemistry. Tissues for immunohistochemistry were placed into OCT and frozen immediately on dry ice following collection and stored at −80°C. Once frozen, OCT blocks of lung and tracheal tissue samples from day 7 postinfection were sectioned and made into slides. Each slide was then fixed with 4% paraformaldehyde, permeabilized with 0.01% Triton X-100, and then incubated with a rabbit polyclonal antibody that recognizes a *B. pertussis* cell surface protein that was provided by Amanda Burnham-Marusich (DxDiscovery, Inc., Reno, NV), followed by incubation with goat anti-rabbit IgG (H+L)-Alexa Fluor 488 secondary antibody, and then stained with rhodamine phalloidin, and staining was completed with DAPI (4′,6-diamidino-2-phenylindole). The stained slides were then visualized using a Nikon Eclipse 90i fluorescence microscope or a Zeiss LSM 710 confocal microscope.

Statistical analysis. All statistical analyses were performed using GraphPad Prism (version 5) software. A nonparametric one-way analysis of variance with Dunn's posttest using naive baboons as the control or a one-sample *t* test using a hypothetical value of 0 with a 95% confidence interval was performed.

ACKNOWLEDGMENTS

We thank Nicole Reuter and Alisha Preno for technical assistance. We thank Drusilla Burns and Susan Brockmeier for critical reading of the manuscript.

This work was funded by the U.S. Food and Drug Administration and NIH/NIAID through interagency agreement Y1-AI-1727-01. Baboons were obtained from the Oklahoma Baboon Research Resource. The Oklahoma Baboon Research Resource was supported by grant numbers P40RR012317 and 5R24RR016556-10 from the National Institutes of Health National Center for Research Resources.

REFERENCES

1. Yeung KHT, Duclos P, Nelson EAS, Hutubessy RCW. 2017. An update of the global burden of pertussis in children younger than 5 years: a modelling study. Lancet Infect Dis 17:974–980. https://doi.org/10.1016/S1473-3099(17)30390-0.
2. Melvin JA, Scheller EV, Miller JF, Cotter PA. 2014. *Bordetella pertussis* pathogenesis: current and future challenges. Nat Rev Microbiol 12:274–288. https://doi.org/10.1038/nrmicro3235.
3. Kilgore PE, Salim AM, Zervos MJ, Schmitt HJ. 2016. Pertussis: microbiology, disease, treatment, and prevention. Clin Microbiol Rev 29:449–486. https://doi.org/10.1128/CMR.00083-15.
4. Pinto MV, Merkel TJ. 2017. Pertussis disease and transmission and host responses: insights from the baboon model of pertussis. J Infect 74(Suppl 1):S114–S119. https://doi.org/10.1016/S0163-4453(17)30201-3.
5. Wood N, McIntyre P. 2008. Pertussis: review of epidemiology, diagnosis, management and prevention. Paediatr Respir Rev 9:201–211. https://doi.org/10.1016/j.prrv.2008.05.010.
6. McIntyre P, Wood N. 2009. Pertussis in early infancy: disease burden and preventive strategies. Curr Opin Infect Dis 22:215–223. https://doi.org/10.1097/QCO.0b013e32832b3540.
7. Paddock CD, Sanden GN, Cherry JD, Gal AA, Langston C, Tatti KM, Wu KH, Goldsmith CS, Greer PW, Montague JL, Eliason MT, Holman RC, Guarner J, Shieh WJ, Zaki SR. 2008. Pathology and pathogenesis of fatal *Bordetella pertussis* infection in infants. Clin Infect Dis 47:328–338. https://doi.org/10.1086/589753.
8. Sawal M, Cohen M, Irazuzta JE, Kumar R, Kirton C, Brundler MA, Evans CA, Wilson JA, Raffeeq P, Azaz A, Rotta AT, Vora A, Vohra A, Abboud P, Mirkin LD, Cooper M, Dishop MK, Graf JM, Petros A, Klonin H. 2009. Fulminant pertussis: a multi-center study with new insights into the clinico-

pathological mechanisms. Pediatr Pulmonol 44:970–980. https://doi.org/10.1002/ppul.21082.
9. Palvo F, Fabro AT, Cervi MC, Aragon DC, Ramalho FS, Carlotti A. 2017. Severe pertussis infection: a clinicopathological study. Medicine (Baltimore) 96:e8823. https://doi.org/10.1097/MD.0000000000008823.
10. Warfel JM, Beren J, Kelly VK, Lee G, Merkel TJ. 2012. Nonhuman primate model of pertussis. Infect Immun 80:1530–1536. https://doi.org/10.1128/IAI.06310-11.
11. Warfel JM, Beren J, Merkel TJ. 2012. Airborne transmission of *Bordetella pertussis*. J Infect Dis 206:902–906. https://doi.org/10.1093/infdis/jis443.
12. Kapil P, Papin JF, Wolf RF, Zimmerman LI, Wagner LD, Merkel TJ. 2018. Maternal vaccination with a monocomponent pertussis toxoid vaccine is sufficient to protect infants in a baboon model of whooping cough. J Infect Dis 217:1231–1236. https://doi.org/10.1093/infdis/jiy022.
13. Warfel JM, Papin JF, Wolf RF, Zimmerman LI, Merkel TJ. 2014. Maternal and neonatal vaccination protects newborn baboons from pertussis infection. J Infect Dis 210:604–610. https://doi.org/10.1093/infdis/jiu090.
14. Warfel JM, Zimmerman LI, Merkel TJ. 2015. Comparison of three whole-cell pertussis vaccines in the baboon model of pertussis. Clin Vaccine Immunol 23:47–54. https://doi.org/10.1128/CVI.00449-15.
15. Warfel JM, Zimmerman LI, Merkel TJ. 2014. Acellular pertussis vaccines protect against disease but fail to prevent infection and transmission in a nonhuman primate model. Proc Natl Acad Sci U S A 111:787–792. https://doi.org/10.1073/pnas.1314688110.
16. Cherry JD, Paddock CD. 2014. Pathogenesis and histopathology of pertussis: implications for immunization. Expert Rev Vaccines 13:1115–1123. https://doi.org/10.1586/14760584.2014.935766.
17. Funnell SG, Robinson A. 1993. A novel adherence assay for *Bordetella pertussis* using tracheal organ cultures. FEMS Microbiol Lett 110:197–203. https://doi.org/10.1111/j.1574-6968.1993.tb06320.x.
18. Guevara C, Zhang C, Gaddy JA, Iqbal J, Guerra J, Greenberg DP, Decker MD, Carbonetti N, Starner TD, McCray PB, Jr, Mooi FR, Gomez-Duarte OG. 2016. Highly differentiated human airway epithelial cells: a model to study host cell-parasite interactions in pertussis. Infect Dis (Lond) 48:177–188. https://doi.org/10.3109/23744235.2015.1100323.
19. Soane MC, Jackson A, Maskell D, Allen A, Keig P, Dewar A, Dougan G, Wilson R. 2000. Interaction of *Bordetella pertussis* with human respiratory mucosa in vitro. Respir Med 94:791–799. https://doi.org/10.1053/rmed.2000.0823.
20. Wilson R, Read R, Thomas M, Rutman A, Harrison K, Lund V, Cookson B, Goldman W, Lambert H, Cole P. 1991. Effects of *Bordetella pertussis* infection on human respiratory epithelium in vivo and in vitro. Infect Immun 59:337–345.
21. Mallory FB, Hornor AA. 1912. Pertussis: the histological lesion in the respiratory tract. J Med Res 27:115–124-3.
22. Warfel JM, Merkel TJ. 2013. *Bordetella pertussis* infection induces a mucosal IL-17 response and long-lived Th17 and Th1 immune memory cells in nonhuman primates. Mucosal Immunol 6:787–796. https://doi.org/10.1038/mi.2012.117.
23. Dunne A, Ross PJ, Pospisilova E, Masin J, Meaney A, Sutton CE, Iwakura Y, Tschopp J, Sebo P, Mills KH. 2010. Inflammasome activation by adenylate cyclase toxin directs Th17 responses and protection against *Bordetella pertussis*. J Immunol 185:1711–1719. https://doi.org/10.4049/jimmunol.1000105.
24. Misiak A, Leuzzi R, Allen AC, Galletti B, Baudner BC, D'Oro U, O'Hagan DT, Pizza M, Seubert A, Mills KHG. 2017. Addition of a TLR7 agonist to an acellular pertussis vaccine enhances Th1 and Th17 responses and protective immunity in a mouse model. Vaccine 35:5256–5263. https://doi.org/10.1016/j.vaccine.2017.08.009.
25. Wilk MM, Misiak A, McManus RM, Allen AC, Lynch MA, Mills KHG. 2017. Lung CD4 tissue-resident memory T cells mediate adaptive immunity induced by previous infection of mice with *Bordetella pertussis*. J Immunol 199:233–243. https://doi.org/10.4049/jimmunol.1602051.
26. Misiak A, Wilk MM, Raverdeau M, Mills KH. 2017. IL-17-producing innate and pathogen-specific tissue resident memory gammadelta T cells expand in the lungs of *Bordetella pertussis*-infected mice. J Immunol 198:363–374. https://doi.org/10.4049/jimmunol.1601024.
27. Ryan M, Murphy G, Gothefors L, Nilsson L, Storsaeter J, Mills KH. 1997. *Bordetella pertussis* respiratory infection in children is associated with preferential activation of type 1 T helper cells. J Infect Dis 175:1246–1250. https://doi.org/10.1086/593682.
28. Mascart F, Verscheure V, Malfroot A, Hainaut M, Pierard D, Temerman S, Peltier A, Debrie AS, Levy J, Del Giudice G, Locht C. 2003. *Bordetella pertussis* infection in 2-month-old infants promotes type 1 T cell responses. J Immunol 170:1504–1509. https://doi.org/10.4049/jimmunol.170.3.1504.
29. Hafler JP, Pohl-Koppe A. 1998. The cellular immune response to *Bordetella pertussis* in two children with whooping cough. Eur J Med Res 3:523–526.
30. National Research Council. 2011. Guide for the care and use of laboratory animals, 8th ed. National Academies Press, Washington, DC.